

Varistor characteristics in PTCR-type (Ba,Sr)TiO₃ ceramics prepared by single-step firing in air

M. KUWABARA and H. MATSUDA

Department of Materials Science, The University of Tokyo, 7-3-1 Hongo, Tokyo 113, Japan

Y. OHBA

Taiko Refractories Co., Tobata, Kitakyushu 804, Japan

E-mail: Kuwabara@ptcr.mm.t.u-tokyo.ac.jp

This paper deals with donor, acceptor-codoped (Ba_{0.4}Sr_{0.6})TiO₃ ceramics with distinct varistor characteristics at room temperature, which were prepared by single-step firing in air. The materials, with the Curie point at around -90°C , exhibited a large PTCR (positive temperature coefficient of resistivity) effect of more than seven orders of magnitude in the temperature range -90°C (the resistivity $\rho \approx 10^3 \Omega \cdot \text{cm}$) to room temperature ($\rho > 10^{10} \Omega \cdot \text{cm}$). An apparent dielectric constant of >20000 and $\tan \delta < 0.05$ (at 100 kHz) were observed for the present materials at room temperature, and moreover, the materials exhibited nonlinear current-voltage characteristics with the nonlinear coefficient, α , in the range 7–12 and the varistor field, E_v , in the range 0.3–1.0 kV/cm. The value of α in the present materials increased systematically with increasing ρ in their PTCR temperature range. It has been found that there exists a close correlation between α and the grain-boundary potential barrier height, $e\phi$, obtained from the ρ - T characteristic of the materials. An almost linear relationship was also found to exist between α and $\log E_v$ for the present materials. © 1999 Kluwer Academic Publishers

1. Introduction

Semiconducting ceramics with an insulating interface layer at the grain boundaries are expected to exhibit a nonlinear current (J)-voltage (E) characteristic. The zinc oxide (ZnO) varistor is the most representative one of such semiconducting ceramics, which is well known to show a J - E characteristic with the highest level of nonlinearity in all ceramic varistors [1, 2]. The nonlinearity of J - E curves in varistors can be described by two parameters, that is the nonlinear coefficient, α (in $J = KE^\alpha$; K is a constant), and the varistor field E_v (the electric field at which the behaviour of a J - E curve changes from ohmic ($\alpha = 1$) to nonlinear ($\alpha > 1$)). Since these varistor parameters are generally very sensitive to even small changes of the composition and microstructure in ceramic varistors, great many efforts have been made to establish a way of fabricating ZnO ceramics with well-controlled varistor parameters. Consequently, our understanding of the varistor characteristics in ZnO ceramics, based on the physics and chemistry of the material, has been greatly improved, and it is now possible to produce ZnO ceramics with a varistor characteristic as designed. However, the varistor mechanism in ZnO ceramics is still open. Even the correlation between the varistor parameters, and their dependence upon the grain-boundary barrier height as well, has been little understood yet. This is probably due to the difficulty of producing ZnO varistors with their parameters varied in a systematic way, without changing the basic composition and microstructure. Be-

sides ZnO varistors strontium titanate (SrTiO₃)-based ceramic varistors, with a microstructure similar to that of grain-boundary-barrier-layer (GBBL) capacitor [3], have also been developed as ones providing an excellent varistor function based on their high electric capacitance. Many investigations have been made to clarify the mechanism of this type of varistor too; nevertheless, our understanding of it is still in a poor level particularly regarding the conduction mechanism in an insulating layer with a high dielectric constant.

From microstructural consideration of the above-mentioned varistor ceramics one may recognize that donor-doped barium titanate (BaTiO₃)-based ceramics that exhibit a large positive temperature coefficient of resistivity (PTCR) characteristic with the maximum resistivity at room temperature can be another type of ceramic varistors. It is well known that donor-doped semiconducting BaTiO₃ ceramics exhibit a PTCR anomaly above the Curie point (T_c ; $\approx 120^{\circ}\text{C}$), and the Curie point can be shifted over a wide temperature range (substantially between $\approx -100^{\circ}\text{C}$ and $+480^{\circ}\text{C}$) by compositional modifications. Substituting Sr for Ba lowers the T_c and substituting Pb for Ba increases it. Semiconducting BaTiO₃-based ceramics with their T_c at a temperature in the range of -60 to -90°C are expected to exhibit their maximum resistivity (necessary to be $>10^9 \Omega \cdot \text{cm}$) around room temperature. Donor-doped ceramics with the basic compositions (Ba_{1-x}Sr_x)TiO₃ having a value of x between 0.5 and 0.6 are suitable for the purpose. There have been a few reports on the

preparation and varistor characteristics of such BaTiO_3 -based ceramics, which were produced by using a single-step firing involving a reduction-reoxidation process [4, 5], in which, however, no quantitative analysis of the varistor characteristics observed was made. Recently, we have succeeded in producing $(\text{Ba}_{0.4}\text{Sr}_{0.6})\text{TiO}_3$ ceramics with a distinct varistor characteristic at room temperature by single-step firing in air (involving no reduction process at all), and moreover, we found the fact that the α value of the materials has close relationships with both E_v and the grain-boundary barrier height, $e\phi$, in the PTCR temperature range of the materials. This paper reports the details of the varistor characteristics obtained for PTCR-type $(\text{Ba}_{0.4}\text{Sr}_{0.6})\text{TiO}_3$ ceramics produced in this study.

2. Experimental

Experimental procedures for preparation of samples and electrical measurements used in this study were reported elsewhere [6]. Commercial high-purity BaTiO_3 and SrTiO_3 (both from Fuji Titanium Industrial Co., Ltd., Tokyo, purity = 99.98%) were used as starting materials. The addition of La (as a donor element) was performed in the form of an aqueous solution. Mn (as an acceptor element) was also added in the form of an aqueous solution. An aqueous solution of La was made by first dissolving La_2O_3 in HNO_3 and then diluted with water, followed by evaporating excess HNO_3 . A Mn aqueous solution was also prepared in the same way, where Mn metal was used and dissolved in HNO_3 . Required amounts of the La (0.3 at %) and Mn (0.025 at %) solutions and excess TiO_2 (0.0, 0.5, 1.0 and 5.0 mol %) as a sintering aid were added to the mixed powders of BaTiO_3 and SrTiO_3 with the composition $(\text{Ba}_{0.4}\text{Sr}_{0.6})\text{TiO}_3$ ($T_c \approx -90^\circ\text{C}$ [7]; BSTO, hereafter), and the mixtures were then mixed well using wet ball-milling. After drying, the mixed powder was pressed into pellets, followed by sintering at 1450°C for 5 h in air to yield sintered bodies. All the obtained ceramic materials had a relative sintered density in the range 93 to 95% (except for the material with TiO_2 of 5.0 mol %, which had a relative density around 90%) and a microstructure consisting of grains in the range 5 to 20 μm (the material with 5.0 mol % TiO_2 had a rather wide distribution of grain size). One may recognize that the sintered densities of these ceramic materials produced are relatively low, but a porosity of $>5\%$ is necessary to provide barium titanate ceramics with a large PTCR effect via reoxidation during the cooling process [8]. Grain structures of the materials were examined by a scanning electron microscope (SEM).

Electrical measurements were conducted on the obtained materials using a two-probe method with In-Ga alloy electrodes. Resistivity (ρ)-temperature (T) characteristics of the materials (at a voltage in the ohmic bias region) were obtained in the temperature range -200 to 250°C , and J - E characteristics were measured in the temperature range -20 to 80°C (within their PTCR temperature range) using a programmable pA meter (HP-4140B). In the measurements of J - E characteristics, pulsed biases (according to the user's guide of the instrument used) were used to avoid an undesirable

increase in the temperature of the materials due to Joule heating during the measurements. Capacitance measurements (in the frequency range 1 kHz–1 MHz) were also conducted on the materials in the temperature range -20 to 100°C using an impedance meter (HP-4192A). Since no unusual frequency dependence of the capacitance measured was observed, the data obtained at 100 kHz are presented as representative ones in this paper.

3. Results and discussion

Fig. 1 shows the ρ - T characteristics of BSTO samples produced in this study, in which the characteristic of a BSTO sample with 0.5 mol % TiO_2 is not shown since it was found to be almost the same as that of the sample without addition of TiO_2 . Also, the J - E characteristics of the same BSTO samples at room temperature, together with that of a BSTO sample with 0.5 mol % TiO_2 , are shown in Fig. 2, in which the data are given in a plot of $\log J$ versus $\log E$. Fig. 2 indicates that all

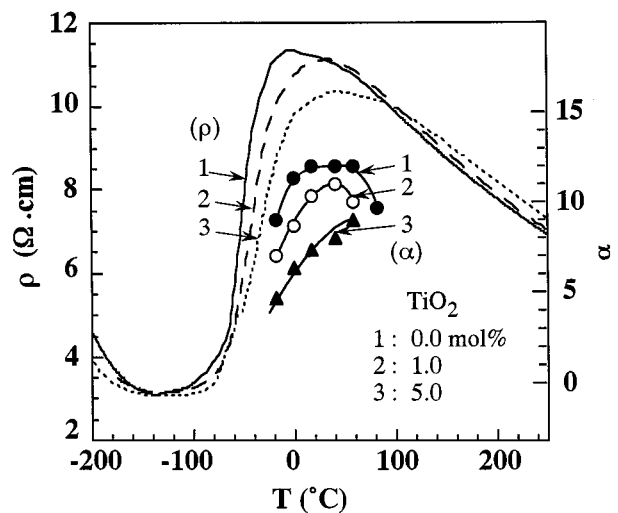


Figure 1 Resistivity-temperature characteristics of $(\text{Ba}_{0.4}\text{Sr}_{0.6})\text{TiO}_3$ ceramics with 0.0, 1.0 and 5.0 mol % TiO_2 added. The nonlinear coefficient, α , of current-voltage characteristics for the materials, obtained in the temperature range -20 to 80°C , is also shown.

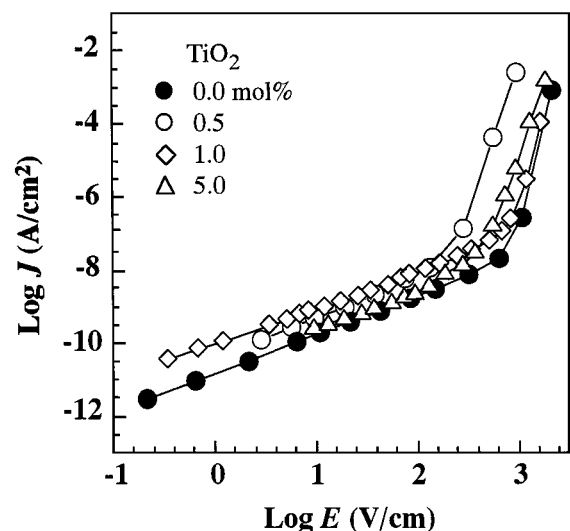


Figure 2 Current-voltage characteristics at room temperature of $(\text{Ba}_{0.4}\text{Sr}_{0.6})\text{TiO}_3$ ceramics with various amounts of TiO_2 added.

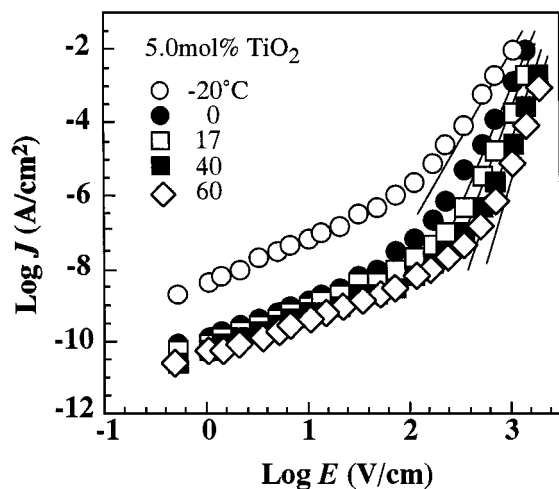


Figure 3 Current-voltage characteristics for a sample with 5.0 mol % TiO₂ added, obtained at several temperatures within the PTCR temperature range of the material.

the BSTO samples exhibited a distinct nonlinear J - E characteristic above a critical electric field (this field is here referred to as the varistor field E_v , though this term is also used to indicate the field specified at a current density of $1\text{mA}/\text{cm}^2$ [1, 2]). The nonlinear coefficient, α , given as the highest slope of a J - E curve in the high field region in this paper, was obtained for each of the BSTO samples in the temperature range -20 to 80°C . As an example of such measurements, J - E characteristics for the sample with 5.0 mol % TiO₂ obtained at various temperatures are shown in Fig. 3. The straight lines drawn on the curves in the high field region are for obtaining the values of α and E_v . The obtained results (that is changes of the α value with temperature for BSTO samples) are simultaneously shown in Fig. 1.

One may recognize that there seems to exist a specific correlation between the values of α and ρ of the present materials, as seen from the data of Fig. 1. This means in other words that a certain correlation exists between α and the grain-boundary barrier height $e\phi$, if allowed to assume that the ρ of the materials can be expressed as $\rho = \rho_0 \exp(e\phi/kT)$, where ρ_0 is a constant (corresponding to the resistivity of the grain bulk). This will be discussed later in more detail. Moreover, it is worthy to note that the value of α decreased rapidly as temperature increased beyond the maximum resistivity temperature of the materials. This fact may suggest that the origin of the varistor property in the materials is closely connected with a conduction current by field-enhanced thermal excitation of trapped electrons into the conduction band at the grain-boundary interface layer, which can be significantly affected by the density and distribution morphology of interface trap levels (or surface acceptor states). This model is completely different from that for the ZnO varistor, in which tunnelling current is now widely accepted as one most appropriately interpreting the varistor mechanism [9].

Fig. 4 shows the temperature dependence of apparent dielectric constant (ϵ_r) for the BSTO samples with 0.0, 0.5, 1.0 and 5.0 mol % TiO₂. This figure indicates that the addition of a small amount of TiO₂ (<0.5 mol %) yielded BSTO materials with an apparent dielectric

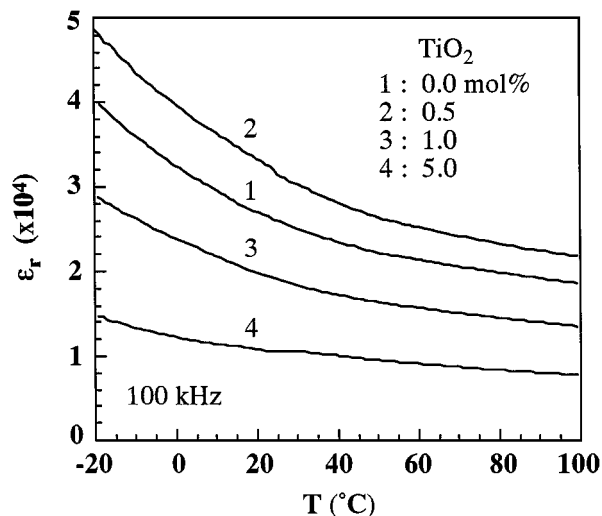


Figure 4 Temperature dependence of apparent dielectric constant for samples with 0.0, 0.5, 1.0 and 5.0 mol % TiO₂, measured at 100 kHz.

constant of >20000 at room temperature, but the excess addition of it (>1.0 mol %) resulted in a degraded dielectric constant. In fact, it can be seen that the material with 5.0 mol % TiO₂ showed a dielectric constant as small as 12000 at room temperature. Since the apparent dielectric constant of GBL capacitors is closely related to their microstructure, we examined the grain structures for some of the present samples. Fig. 5 shows typical SEM microstructures of BSTO materials with 0.0, 1.0 and 5.0 mol % TiO₂ produced in this study, clearly indicating a systematic decrease in grain size with an increase in the amount of TiO₂ added. From these results it may be reasonable to conclude that the decrease in the apparent dielectric constant of the materials with increasing TiO₂ is attributed to a decrease in grain size, that is an increase in the number of grain boundaries per length. As to a considerably small dielectric constant for the sample with 5.0 mol % TiO₂, its rather large porosity ($\approx 10\%$) can be considered to be also responsible for that. On the other hand, a slightly increased dielectric constant for the material with 0.5 mol % TiO₂ seems to result from a change in the grain boundary structure of the material, since any particular increase in grain size was not observed for the material. Here, the effective thickness of the grain boundary layer and the space charge density and its distribution there can be thought to be important factors characterizing the grain boundary structure. Furthermore, it is worthy to note that all the BSTO samples of Fig. 4 exhibited a dielectric loss ($\tan \delta$) of $<3\%$ over the whole temperature range -20 to 100°C .

In Fig. 6 are shown the relationships between α and $e\phi$ obtained for the BSTO samples with 0.0, 1.0 and 5.0 mol % TiO₂ in their PTCR temperature range, indicating that an α value of 12 was attained for the sample with no additive. The value of $e\phi$ was obtained by assuming that the ρ of the materials can be expressed by the equation $\rho = \rho_0 \exp(e\phi/kT)$, as already mentioned above. Here, we used the ρ value at -100°C ($\approx 10^3 \Omega \cdot \text{cm}$) for all the BSTO materials (see the ρ - T curves of Fig. 1) as ρ_0 in the equation for calculation of the value of $e\phi$. It should be noted that since the

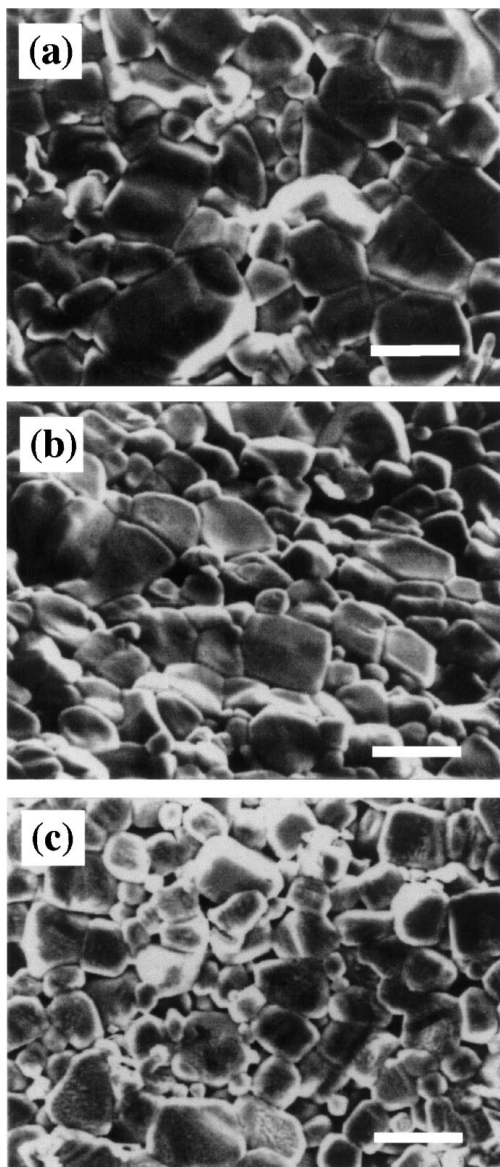


Figure 5 SEM photographs of BSTO ceramics with (a) 0.0, (b) 1.0 and (c) 5.0 mol % TiO₂. Bars indicate 20 μm .

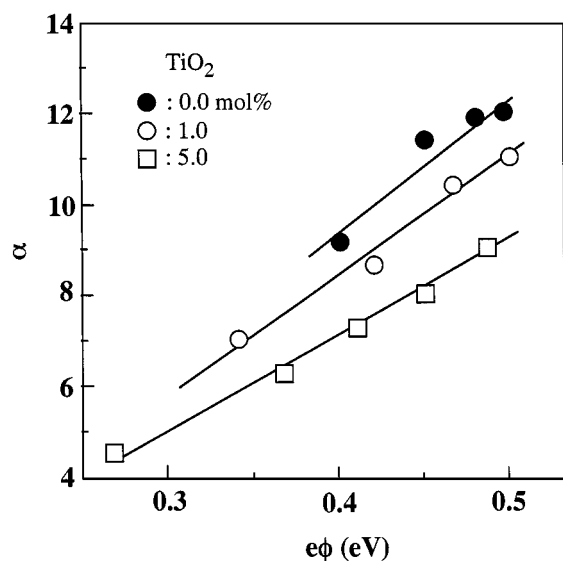


Figure 6 Relationship between α and $e\phi$ obtained for the present samples.

existence of a potential barrier at grain boundaries in BSTO materials even at -100°C has been confirmed [6], the value of $10^3 \Omega \cdot \text{cm}$ is actually not equal to the value of the bulk resistivity of the present materials. However, this residual barrier height was not taken into account here, because the height of the potential barriers, if it exists, can be estimated to be less than 0.08 eV (taking the true bulk resistivity to be 5–10 $\Omega \cdot \text{cm}$ from results in the previous study [6]) at this temperature. It is obvious from Fig. 6 that the relationship between α and $e\phi$ for the samples can be described well by a straight line with an increased slope with increasing amount of TiO₂ added. It should be noted, however, that such a relationship does not exist any more between the parameters obtained at temperatures above their maximum resistivity temperature as also seen from the data of Fig. 1. Although we have no definite idea to interpret the obtained experimental results, it may be possible to conclude that simple diffusion current passing through a double Schottky-type barrier (first proposed by Heywang [10]) formed at grain boundaries is not responsible for the varistor properties in the present materials. The conduction mechanism based on the Heywang model can explain an α value of <6 , according to the calculation of Mallick, and Emtage [11], but such large α values of >10 as observed for the present materials are difficult to be explained by the model. Tentatively, we thus conclude that the conduction mechanism through surface states at the grain-boundary interface layer is the most likely one for the occurrence of the varistor function in BSTO materials.

Similar plots were made in order to clear the correlation between α and $\log E_v$. The results are shown in Fig. 7, which indicates that E_v values between 0.2 ($\log E_v = 2.3$) and 1 kV/cm ($\log E_v = 3.0$) were observed for the present samples. Here, the field of 1kV/cm corresponds to about 1 V per grain boundary (the present samples had an average grain size around 10 μm). From this figure the relationships between α and $\log E_v$ for the BSTO samples seem to be

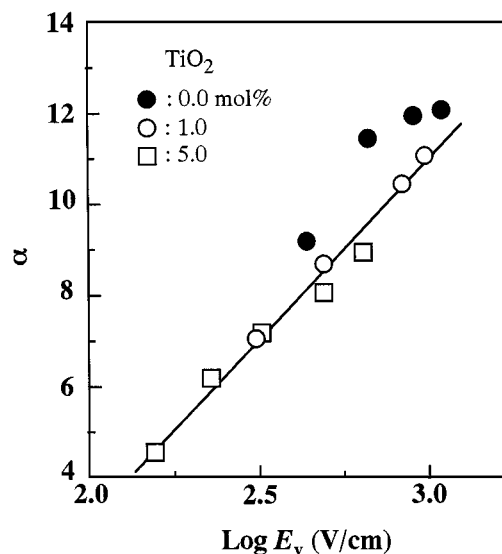


Figure 7 Relationship between α and $\log E_v$ obtained for the present samples.

represented as if by a single straight line irrespective of the amount of TiO₂ added, in contrast to the relationship between α and $e\phi$, which is shown in Fig. 6. Although the data points for the sample with no additive in Fig. 7 are obviously away from the straight line, it is no doubt that there exists an almost linear relationship between the two varistor parameters at least. The data of Fig. 7 indicate at the same time that an α value of >20 is not attainable for BSTO varistors, unless BaTiO₃-based materials with a varistor function based on a completely different varistor mechanism from that in the present materials are produced. We cannot interpret quantitatively at present the linear relationships among the varistor parameters and $e\phi$ observed in this study, but it may be reasonable to conclude that the varistor mechanism in the present materials is completely different from that for the ZnO varistor from the point of view of the α value. In relation to the value of α for BaTiO₃-based materials, there has been work by Kutty *et al.* [12, 13]. They investigated the electrical properties of BaTiO₃-based semiconducting ceramics, and found that the materials exhibited a J - E curve with an α value of >30 at temperatures above their T_c . Although Kutty *et al.* and we used similar systems of materials, the mechanisms of the varistor functions investigated by the two groups are completely different from each other. Kutty *et al.* assumed the occurrence of thermal transition of the grain boundary phase under application of electric biases (by Joule heating), resulting in the formation of a tetragonal-cubic mixed grain structure with a potential barrier at the grain interface. They described the energy band structure of the potential barrier formed as one similar to the metal-insulator-semiconductor structure (known as the MIS [14] structure). Based on this assumption, they interpreted the varistor characteristics observed by essentially the same transport mechanism (by tunnelling current) that is widely accepted for the varistor mechanism in the ZnO varistor. The J - E characteristics in the present materials observed, however, did not show any features of tunnelling current.

4. Conclusion

PTCR-type (Ba_{0.4}Sr_{0.6})TiO₃ ceramics, which exhibited a distinct varistor characteristic at room temperature, have been prepared by firing in a single step in air. The obtained materials, with their T_c around -90°C ,

showed a PTCR effect of more than seven orders of magnitude with a resistivity of $>10^{10} \Omega \cdot \text{cm}$ and a high apparent dielectric constant of >20000 at room temperature. Some of the materials exhibited a nonlinear J - E characteristic with an α value of >10 at room temperature. The value of α obtained for the present materials in their PTCR temperature range was plotted as functions of the potential barrier height, $e\phi$, and the varistor field E_v . The obtained results clearly demonstrate that there exist almost linear relationships between the values of α and $\log E_v$ and also between α and $e\phi$. Although we have no quantitative interpretation at present for these phenomena observed, it must be useful to make the relationship between the varistor parameters clear to better understand the varistor mechanism in ceramic varistors.

Acknowledgement

The financial support of the Ministry of Education, Science and Culture of Japan in the form of the Grant-in-Aid for Scientific Research, no. 08555155 is acknowledged.

References

1. L. M. LEVINSON and H. R. PHILIPP, *Ceram. Bull.* **65** (1986) 639.
2. T. K. GUPTA, *J. Amer. Ceram. Soc.* **73** (1990) 1817.
3. N. YAMAOKA, *Ceram. Bull.* **65** (1986) 1149.
4. T. ITHO, S. TASHIRO and H. IGARASHI, *Jpn. J. Appl. Phys.* **32** (1993) 4261.
5. T. ISHIYA, S. TASHIRO and H. IGARASHI, *ibid.* **34** (1993) 5309.
6. N. TSUDA and M. KUWABARA, *J. Ceram. Soc. Jpn.* **103** (1995) 1006.
7. B. JAFFE, W. R. COOK, JR. and H. JAFFE, in "Piezoelectric Ceramics" (Academic Press, London, 1971) p. 94.
8. M. KUWABARA, *J. Amer. Ceram. Soc.* **64** (1981) 639.
9. K. EDA, *IEEE Electrical Ins. Mag.* **5** (1989) 28.
10. W. HEYWANG, *J. Amer. Ceram. Soc.* **47** (1964) 484.
11. G. T. MALLICK, JR. and P. R. EMTAGE, *J. Appl. Phys.* **39** (1968) 3088.
12. T. R. N. KUTTY and V. RAVI, *Appl. Phys. Lett.* **59** (1991) 2691.
13. *Idem.*, *Mater. Sci. Eng. B* **20** (1993) 271.
14. S. M. SZE, in "Physics of Semiconductor Devices," 2nd ed. (John Wiley & Sons, New York, 1981) p. 362.

Received 19 September 1997

and accepted 14 January 1999